Perpendicular magnetocrystalline anisotropy energy (MAE) of 111-surface slab of Fe_2CoAl

Materials Research Express

OPEN ACCESS

RECEIVED
1 May 2020

ACCEPTED FOR PUBLICATION
29 May 2020

PUBLISHED
5 June 2020

PAPER

Perpendicular magnetocrystalline anisotropy energy (MAE) of 111-surface slab of Fe_2CoAl

Lalrinkima[1,3], L A Fomin[2], I V Malikov[2], Lalthakimi Zadeng[1] and D P Rai[3]

[1] Department of Physics, Mizoram University Aizawl 796009, India
[2] Institute of Microelectronics Technology and High Purity Materials RAS, 142432 Chernogolovka, Russia
[3] Physical Sciences Research Center (PSRC), Department of Physics, Pachhunga University College Aizawl 796001, India

E-mail: dibya@pucollege.edu.in

Keywords: GGA, GGA+U, magnetocrystalline anisotropy energy, spin orbit coupling, band structure

Abstract

We have analyzed the surface stability of different orientations(111, 001, 011) of Fe_2CoAl (FCA) slabs. Among all the slabs, the orientation with 111-surface is found to be most stable with minimum energy. The surface electronic and magnetic properties along with the atomic orbital resolved magneto-crystalline anisotropy energy (MAE) has been performed by using first principles density functional theory (DFT). We have reported the surface metallicity with dispersed electronic bands around the fermi energy (E_F) in all the three terminals Fe/Co/Al. This may be the result of translational broken symmetry in which metallic bonds are broken with the release of free conducting electrons on the surface. We have observed the presence of both the in-plane MAE and the out-plane MAE characterized by the distribution of total MAE over an atomic sites for each Al-, Co- and Fe-terminal. The total MAE favors in-plane magnetization in case of antiferromagnetic configured Al-terminal (MAE = 0.034 meV) and Fe-terminal (0.68 meV) whereas out-plane total MAE is observed in ferromagnetic configured Co-terminal.

1. Introduction

The magnetic materials with half-metallic, large perpendicular magnetic anisotropy, high thermal stability and low critical current, magnetic damping etc, always fascinates the scientific research due to their potential application in spintronics. They also possess high magnetization density, high density spin transfer torque under applied magnetic field which are crucial for implementation in magnetic random access memory (STT-MRAM) and logic devices [1–4]. For materials to device applications size compatibility with preserving the functional properties are always an issue. In most cases, the half-metallicity and other physical properties are destroyed when cleaveged to low dimension surface slab and 2D thin film from the bulk materials. The nano-scale object loses its magnetic stability with the lowering of size scaled [5]. The stabilization of surface magnetization and magnetic crystalline anisotropy of the magnetic materials at its nano-scale, thin film and surface level for successful device application is an outmost challenge. In tetragonal Heusler compounds large magneto-crystalline anisotropy can be easily produced by positioning the Fermi energy at the van Hove singularity in one of the spin channels, while the ferromagnetic cubic Heusler alloys exhibit small magneto-crystalline anisotropy energy (MAE) mainly due to the higher dominating magnetization [6]. So for that reason, the usage of low magnetization materials such as ferrimagnetic and antiferromagnetic materials with large MAE preferred over highly magnetized ferromagnetic materials to reduce critical current density and enhanced the thermal stability in magnetic tunnel junctions (MTJs) [7, 8]. Several results of high values of MAE has been reported in the metal-semiconductor hetero-junction. For example, full Heusler alloy and semiconductor heterostructure (Co_2FeAl)|MgO have been found to exhibit large interfacial perpendicular magnetic anisotropy energy (PMA) value of 1.31 mJ m^{-2} [3], 1.28mJ m^{-2} [9] for Co-terminated in Co_2FeAl|MgO interfaces and a PMA value of 0.428 erg cm^{-2} for FeAl-terminal [10]. Wen *et al* [11] experimentally achieved PMA densities around

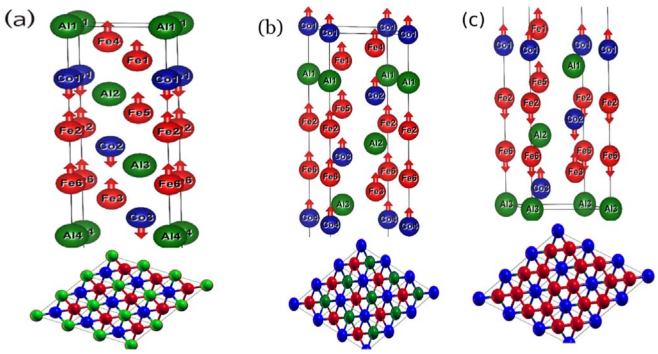

Figure 1. Conventinal slab model (Top-view and Side-view) for (a) Antiferromagnetic (AFM1) Al-terminal (b) Ferromagnetic Co-terminal and (c) Antiferromagnetic(AFM2) Fe-terminal.

2–3 $\times$ 10^6erg cm^{-3} within CFA|MgO and MgO|CFA structures. Interestingly, a large negative perpendicular uniaxial anisotropy has also been observed in CFA|Mgo(001) [12].

In this paper, we have presented the surface electronic and perpendicular magnetic anisotropy energy (PMA) for non-periodic slab (111) of inverse (XA-type) cubic full Heusler alloy Fe_2CoAl. To the best of our knowledge, neither experimental nor theoretical studied have been performed for PMA of free standing Fe_2CoAl 111-surface. However, numbers of work on the analogous composite $L2_1$ structured Co_2FeAl have already been reported. For electronic structure calculation, we have treated strongly correlated electron-electron interaction by including Hubbard parameter (U) [13] (U_{Fe} = 3.82 eV and U_{Co} = 3.89 eV) as GGA+U calculation in addition to GGA.

2. Computational detail

Different FCA surface slabs with orientations [(001), (110), (111)] have been cleavage from the cubic bulk Fe_2CoAl with lattice constant a = 5.703 Å[14]. A vacuum of 15 (Å) is applied along the z-axis to avoid periodic layer interactions. We have performed the first principles DFT [15] calculation using Quantum Espresso (QE) [16] package considering the electron exchange energy within the generalized gradient approximation (GGA) proposed by Perdew–Burke–Ernzerhof(PBE) [17]. We used 250 Rydberg for the kinetic cut off energy and a mesh of 16 $\times$ 16 $\times$ 1 within Monkhorst pack [18] for K-point to integrate the first Brillouin zone. Stuctural relaxation was achieved with a force tolerance of 0.0136eV/Å. We deployed the force theorem [5] as implemented in QE; by performing the self-consistent-field calculation (SCF) without the spin–orbit coupling (SOC) within the scalar pseudopotentials method we obtained the charge density and spin magnetic moment. Then, two types non-SCF calculation are executed with the spin polarized fully relativistic pseudopotentials (with SOC). In which we have considered spin moment with angle 0° in xy-plane for parallel and 90° in z-axis for perpendicular direction. The difference of the band energy between the two spin moment directions (90° and 0°) is the the total MAE.

3. Results and discussion

Among the three different slab orientations (001, 110 and 111) the 111-surface slab with thirteen atomic monolayers have been found to be the most stable with the minimum ground state energy. We have performed the magnetic configuration dependent ground state energy calculation from the 111-surface slab. The 111-surface slabs of Fe_2CoAl are again categorized with three different terminal atoms like Fe-, Co- and Al-terminals as shown in figure 1. The seven magnetic configurations are considered including one ferromagnetic (FM) and six types of antiferromagnetic (AFM) orientations (see tables 1, 2, 3) for each Fe-, Co and Al-terminal, respectively. In terms of their minimum ground state energy with corresponding magnetic configurations; Al-terminal is stable with AFM1-configuration, Fe-terminal with AFM2 configuration and Co-terminal with FM configuration (see tables 1, 2, 3).

3.1. Electronic and magnetic properties

In figures 2, 3, we have presented the spin-resolved partial density of states (DOS) and energy band stuctures of 111-surface slab of Fe_2CoAl, calculated from GGA and GGA+U (U_{Fe} = 3.82 eV and U_{Co} = 3.89 eV) [13] to study the electronic properties. For each terminal, we considered the surface-, subsurface1- and subsurface2

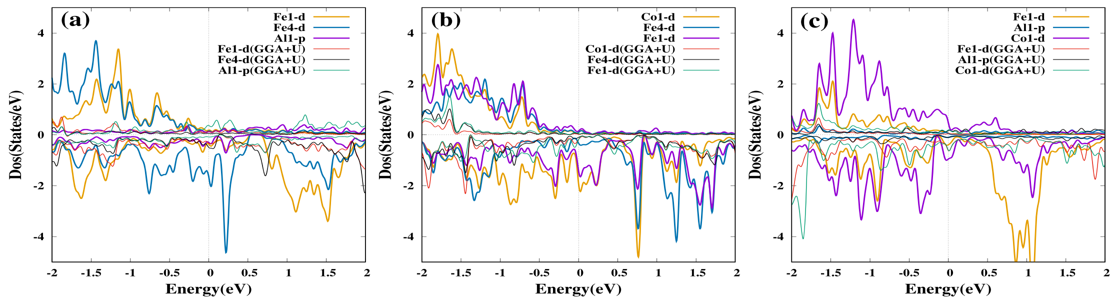

Figure 2. Calculated partial DOS of Fe_2CoAl from GGA and GGA+U: (a) Al-terminal, (b) Co-terminal and (c) Fe-terminal.

Table 1. Magnetic Configuration on magnetic atomic sites (six Fe- and three Co-atoms) and energy difference (E_{FM}-E_{AFM}) in Ry for Al-terminated surface.

Config.	Fe1	Fe2	Fe3	Fe4	Fe5	Fe6	Co1	Co2	Co3	E_{FM}-E_{AFM}(Ry)
FM	↑	↑	↑	↑	↑	↑	↑	↑	↑	0.00
AFM1	↑	↑	↑	↑	↑	↑	↓	↓	↓	0.009
AFM2	↑	↓	↑	↓	↑	↓	↑	↓	↑	−0.040
AFM3	↑	↑	↓	↓	↑	↑	↑	↑	↓	−3.889
AFM4	↓	↓	↑	↑	↓	↓	↓	↓	↑	−2.438
AFM5	↑	↓	↓	↑	↓	↓	↑	↓	↓	−0.004
AFM6	↓	↑	↑	↓	↑	↑	↓	↑	↑	−0.004

Table 2. Magnetic Configuration on magnetic atomic sites (six Fe- and four Co-atoms) and energy difference (E_{FM}-E_{AFM}) in Ry for Co-terminated surface.

Config.	Fe1	Fe2	Fe3	Fe4	Fe5	Fe6	Co1	Co2	Co3	Co4	E_{FM}-E_{AFM}(Ry)
FM	↑	↑	↑	↑	↑	↑	↑	↑	↑	↑	0.000
AFM1	↑	↑	↑	↑	↑	↑	↓	↓	↓	↓	−4.762
AFM2	↑	↓	↑	↓	↑	↓	↑	↓	↑	↓	−6.889
AFM3	↑	↑	↓	↓	↑	↑	↑	↑	↓	↓	−5.101
AFM4	↓	↓	↑	↑	↓	↓	↓	↓	↑	↓	−3.690
AFM5	↑	↓	↓	↑	↓	↓	↑	↓	↓	↑	−4.798
AFM6	↓	↑	↑	↓	↑	↑	↓	↑	↑	↓	−4.797

Table 3. Magnetic Configuration on magnetic atomic sites (seven Fe- and three Co-atoms) and energy difference (E_{FM}-E_{AFM}) in Ry for Fe-terminated surface.

Config.	Fe1	Fe2	Fe3	Fe4	Fe5	Fe6	Fe7	Co1	Co2	Co3	E_{FM}-E_{AFM}(Ry)
FM	↑	↑	↑	↑	↑	↑	↑	↑	↑	↑	0.000
AFM1	↑	↑	↑	↑	↑	↑	↑	↓	↓	↓	−0.314
AFM2	↑	↓	↑	↓	↑	↓	↑	↑	↓	↑	3.551
AFM3	↑	↑	↓	↓	↑	↑	↓	↑	↑	↓	−0.678
AFM4	↓	↓	↑	↑	↓	↓	↑	↓	↓	↑	2.586
AFM5	↑	↓	↓	↑	↓	↓	↑	↑	↓	↓	3.520
AFM6	↓	↑	↑	↓	↑	↑	↓	↓	↑	↑	−2.105

atomic layer to reveal the electronic properties. We observed a metallic behaviour in both the spin channels with dispersed bands around the fermi level due to the breaking of metallic bonding when the non-periodic surface slab is cleavaged from the periodic bulk system and also the DOS decreases from GGA to GGA+U calculation in all cases (See figures 2(a), (b) and (c)). In Al-terminated surface, as shown in figure 2(a), all the Fe1-*d*, Al-*p* and Fe4-*d* spin-up and spin-down states are dispersed around the Fermi level (E_F) within GGA and GGA+U calculation. The higher occupation of Fe4-*d* states prior to Fe1-*d* states around the E_F in the spin-down channel may be due to the absence of $d - d$ hybridization between Fe4-*d* and Fe1 -*d* states. A higher peak of Fe4-*d* spin down states likely reveals the surface reconstruction [19, 20]. Interestingly, we observed a small spin-down band gap (0.19 eV) between 0.55 eV–0.74 eV in the conduction band from GGA calculation. By treating electron-

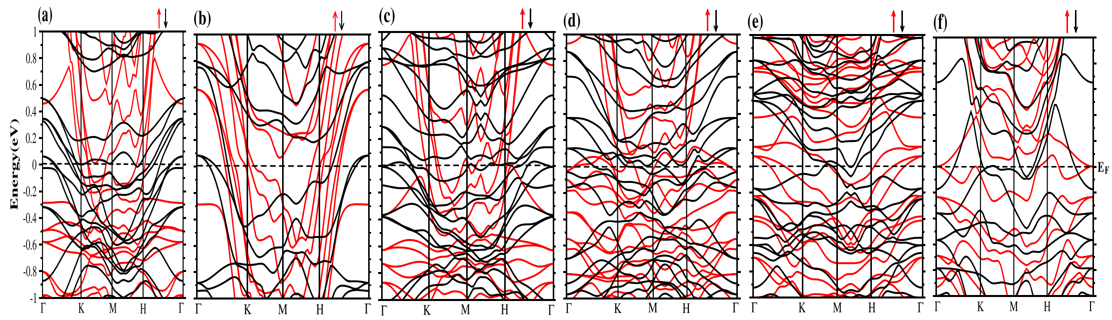

Figure 3. Calculated band structures:(a) Al-terminal(GGA), (b) Al-terminal(GGA+U), (c) Co-terminal(GGA), (d) Co-terminal(GGA +U), (e) Fe-terminal(GGA) and (f) Fe-terminal(GGA+U).

Table 4. Comparision between surface/subsurface atomic sites magnetic moment with their corresponding moment in the bulk Fe_2CoAl.

	Atomic site	μ_B (GGA)	μ_B (GGA+U)
Al-terminal	Fe4	2.45	2.68
	Fe1	2.43	2.53
Co-terminal	Co1	1.80	1.90
	Fe4	2.67	2.77
	Fe1	2.25	2.48
Fe-terminal	Fe1	3.00	3.01
	Co1	0.83	1.35
Bulk	Fe1	2.56	2.76
	Fe2	1.64	2.16
	Co	1.18	0.89

electron interactions in GGA+U calculation, free electrons abruptly reduced which results lesser population states. The presence of small hybridization between Co1-*d* and Fe1-*d* in spin-down states results in coupled states at the E_F in FM Co-terminated surface, the similar trend of results are obtained for AFM1 Al-terminated and AFM2 Fe-terminal electronic structure. We have calculated the total spin polarization degree for each terminal using the relation equation (1) [21]

$$P = \frac{N_{\uparrow}(E_F) - N_{\downarrow}(E_F)}{N_{\uparrow}(E_F) + N_{\downarrow}(E_F)} \quad (1)$$

where $N_{\uparrow}(E_F)$ and $N_{\downarrow}(E_F)$ are the densities of states at E_F for spin-up and spin-down channels respectively. We estimated the polarization degree 65% (GGA) and 21.7% (GGA+U) for Al-terminal, 62.4% (GGA) and 36.5% (GGA+U) for Co-terminal, where a comparatively low polarization degree with 40% (GGA) and 5% (GGA+U) for Fe-terminal.

The calculated total magnetic moments are found to be 18.9 μ_B (GGA) and 20.46 μ_B (GGA+U) for ferromagnetic Co-terminal and comparatively higher than antiferromagnetic Al-terminal [5.32 μ_B (GGA) and 9.73 μ_B (GGA+U)] and Fe-terminal [0.03 μ_B (GGA) and 3.5 μ_B (GGA+U)]. The calculated values of magnetic moment of the surfaces, sub-surfaces atoms in each terminals along with the partial magnetic moments of the corresponding magnetic moment of the bulk Fe_2CoAl [14] is shown in Table 4. The moment of Fe4 atoms in sub-surface1 for Al- and Co-terminals are comparable with the moment of Fe1 site in the bulk whereas, the Fe1 moment of the sub-surface2 are likely within the range of Fe1 and Fe2 sites in the bulk stucture. But, the values of magnetic moment of Co1 atom in Co-terminal surface is fractionally higher as compared to that of the Co1 atom at sub-surface1 of the Fe-terminal and the bulk within both GGA and GGA+U calculation. The atomic sites magnetic moment from GGA and GGA+U calculation are also presented in figure 4. The anti-parallely configured three Co-atoms of Al-terminal experienced parallel magnetization along with Fe-atoms from GGA calculation, this may be due to the strong coupling between Co-atoms and Fe-atoms within the core-region of the slab. The magnetic atoms (Fe and Co) in the FM Co-terminal shows parallel magnetization as expected where the moment of magnetic atoms in the AFM2 Fe-terminal oscillate around zero.

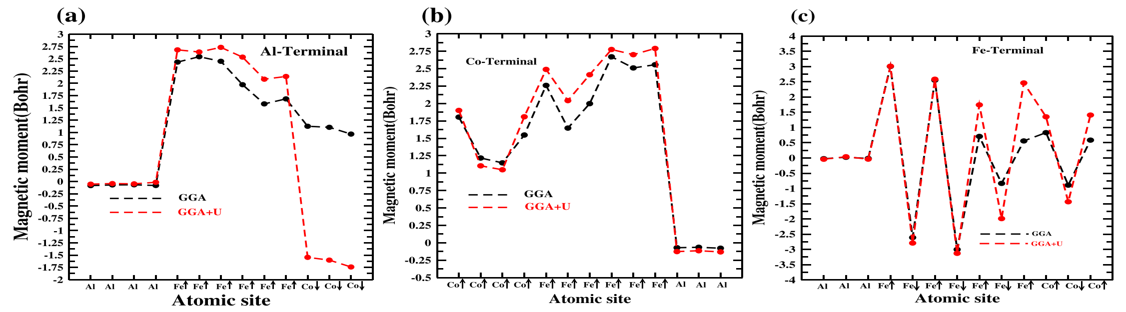

Figure 4. Calculated Atomic site magnetic moment(a) Al-terminal and (b) Co-terminal and (c) Fe-terminal.

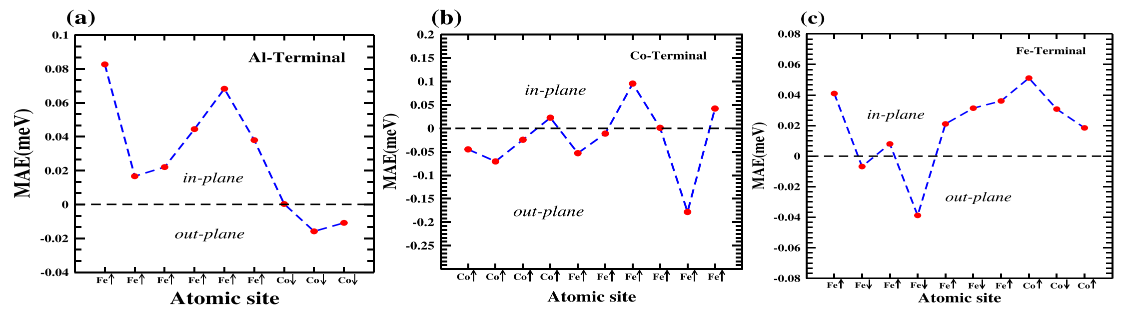

Figure 5. Calculated Atomic resolved MAE (a) Al-terminal and (b) Co-terminal and (c) Fe-terminal.

3.2. Perpendicular Magnetocrystalline anisotropy

We calculated the energy required to switch the magnetization direction from easy(xy)axis to the perpendicular direction(z) of the crystal axis for each terminal, which is usually termed as perpendicular magnetocrystalline anisotropy energy (MAE). We estimated the total in-plane MAE values 0.034 meV/cell and 0.68 meV/cell for the two antiferromagnetic Al(AFM1)- and Fe-(AFM2)terminated surfaces respectively, whereas the out-plane total MAE −0.087 meV/cell for ferromagnetic Co-terminated surface. The distribution of total MAE over an atomic sites i is given by equation (2) [5]

$$MAE_i = \int^{E_F^1} (E - E_F) n_i^1(E) dE - \int^{E_F^2} (E - E_F) n_i^2(E) dE \quad (2)$$

where E_F is the Fermi energy of obtained from non-SCF calculation with SOC and subtracted from all the eigen values to produce correct local decomposition of MAE. Figure 5 shows the atomic resolved MAE for different terminals. In case of antiferromagnetic Al-terminal(AFM1) and Fe-terminal(AFM2), we have noticed the dependence of total MAE on the atomic resolved surface and sub-surfaces. Incase of Co-terminal, the out-plane favours the surface, whereas the sub-surfaces are ferromagnetic. The major contribution to the total out-plane MAE is neither dominated by surface nor by sub-surface atoms rather from the core-region. This may be due to the cancellation between surface and sub-surface atomic moments [5]. Usually the cubic bulk structure exhibit negligibly small MAE per atom, but it is possible to get higher measurable values of MAE (more likely inmeV) in nanostructures [22, 23] due to reducibility of dimension or miniature in sizescale. Unfortunately, we do not have sufficient reported data to compare our results.

4. Conclusion

We have studied the surface electronic and perpendicular magnetocrystalline anisotropy of 111-surface slab of inverse Heusler alloy Fe_2CoAl using the first principles calculation. Adopting the different atomic terminals we have calculated the minimum ground state energy for various magnetic configurations (FM and AFM). The slab with different atomic-terminals and energetically stable ground states are AFM1:Al-terminal, FM:Co-terminal and AFM2:Fe-terminal. All the terminals are magnetic metals with finite value of total magnetic moments and dispersed bands around E_F in both the spin channels from GGA as well as GGA+U approaches. We have observed the decrease in the degree of the total spin polarization from the GGA to GGA+U calculation in all cases. This may be due to the large number of free conducting charges dispersed on the surface and another reason might be the irrelevant choice of the Hubbard potential (U) to incorporate the surface atoms. In fact, we have observed a small spin-down energy gap (0.19 eV) between 0.55 eV–0.74 eV in Al-terminal within GGA calculation. By varying the cell parameters it may be possibly tuned the Fermi level in the spin band gap to get the surface half-metallicity. The perpendicular magnetocrystalline anisotropy energy (PMA) calculation were performed using force theorem as implemented in Quantum Espresso. We observed both in-plane and out-plane mixed-up character for atomic-layer resolved MAE. However, Al- and Fe-terminal favor the in-plane while Co-terminal is subjected to out-plane total MAE.

Acknowledgments

D P Rai acknowledges Department of Science and Technology (DST) New Delhi, Govt. of India vide Lett. No. INT/RUS/RFBR/P-264. Prof. I V Malikov acknowledges Russian Foundation for Basic Research (RFBR), Russia, RFBR-17-57-45024. Obituary to Prof. G M Mikhailov (RAS).

ORCID iDs

Lalrinkima https://orcid.org/0000-0002-3534-7325
D P Rai https://orcid.org/0000-0002-3803-8923

References

[1] Nistor L E, Rodmacq B, Auffret S and Dieny B 2009 Pt/Co/oxide and oxide/Co/Pt electrodes for perpendicular magnetic tunnel junctions *Appl. Phys. Lett.* **94** 012512
[2] Ikeda S, Miura K, Yamamoto H, Mizunuma K, Gan H D, Endo M, Kanai S, Hayakawa J, Matsukura F and Ohno H 2010 A perpendicular-anisotropy CoFeB-Mgo magnetic tunnel junction *Nat. Mater.* **9** 721
[3] Vadapoo R, Halal A, Yang H and Chshiev M 2016 First principle investigation of magnetocrystalline anisotropy at the $L2_1$ full Heusler| MgO interfaces and tunnel junction *Phys. Rev.* B **94** 104418 (5-1)
[4] Malikov I V, Fomin L A, Berezin V A, Chernykh A V, Rai D P and Mikhailov G M 2019 Study of the Fe_2CoAl heusler alloy films growth on the R-plane sapphire substrate by scanning probe microscopy *Ferroelectrics* **541** 79–92
[5] Li D, Barrateau C, Castell M R, Silly F and Smogunov A 2014 Out- versus in-plane magnetic anisotropy of free Fe and Co nanocrystal: Tight-binding and first-principle studies *Phys. Rev.* B **90** 205409 (7-1)
[6] Felser C, Wollman L, Chadov S, Fecher G H and Parkin S P S 2015 Basics and prospective of magnetic Heusler compounds *APL Mater* **3** 041518 (8-1)
[7] Odkhuu D, Rhim S H, Park N, Nakamura K and Hong S C 2018 Jahn-Teller driven perpendicular magnetocrystalline anisotropy in metastable ruthenium *Phys. Rev.* B **98** 094408 (8-1)
[8] Loth S, Baumann S, Lutz C P, Eigler D M and Heinrich A J 2014 Bistability in atomic-scale antiferromagnets *Science* **335** 196–9
[9] Tsujikawa M, Mori D, Miura Y and Shirai M 2013 Perpendicular magnetic anisotropy and its electrical modulation of MgO/Co_2FeAl interface: a first-principles study *Proceeding of MML 2013—The VIII International Symposium on Metallic Multilayers (MML2013) (Kyoto, Japan, May 19-24)*
[10] Bai Z, Shen L, Cai Y, Wu Q, Zeng M, Han G and Feng Y P 2014 Magnetocrystalline anisotropy and its electric-field-assisted switching of Heusler-compound-based perpendicular magnetic tunnel junctions *New J. Phys.* **16** 103033 (18-1)
[11] Wen Z, Sukegawa H, Mitani S and Inomata K 2011 Perpendicular magnetization of Co_2FeAl full Heusler alloy films induced by MgO interface *Appl. Phys. Lett.* **98** 242507 (3-1)
[12] Belmeguenai M, Tuzcuoglu H, Gabor M S, Petrisor T Jr., Tiusan C, Berling D, Zighem F, Chauveau T, Cherif S M and Moch P 2013 Co 2 FeAl thin films grown on MgO substrates: correlation between static, dynamic, and structural propertie *Phys. Rev.* B **87** 184431 (11-1)
[13] Rai D P, Shankar A, Sandeep, Singh L R, Jamal M, Hashemifar S J, Ghimire M P and Thapa R K 2012 Calculation of coulomb repulsion (U) for 3d transition elements in Co2YAl type Heusler alloys *Arm. J. Phys.* **5** 105-110 (http://ajp.asj-oa.am/511/)
[14] Siakeng L, Mikhailov G and Rai D P 2018 Electronic, elastic and x-ray spectroscopic properties of direct and inverse full Heusler compounds Co_2FeAl and Fe_2CoAl, promising materials for spintronic applications: a DFT+U approach *J. Mater. Chem.* C **6** 10341–9
[15] Kohn W and Sham L J 1965 Self-Consistent equations Including Exchange and Correlation Effects *Phys. Rev.* **140** A1133–8
[16] Giannozzi P, Baroni S, Bonini N, Calandra M, Car R, Cavazzoni C, Ceresoli D, Chiarotti G L, Cococcioni M and Dabo I 2009 QUANTUM ESPRESSO: a modular and open-source software project for quantum simulations of materials *J. Phys. Condens. Mat.* **21** 395502
[17] Perdew J P, Burke K and Ernzerhof M 1996 Generalized gradient approximation made simple *Phys. Rev. Lett.* **77** 3865–8
[18] Monkhorst H J and Pack J D 1976 Special points for brillouin zone integrations *Phys. Rev.* B **13** 5188–92
[19] Galanakis I 2002 Surface properties of the half-and full-Heusler alloys *J. Phys.: Condens. Matt.* **14** 6329–40
[20] Paudel R and Zhu J 2019 Investigation of half-metallicity and magnetism of bulk and (111)-surfaces of Fe_2MnP full Heusler alloy *Vacuum* **164** 336–42
[21] Soulen R J Jr *et al* 1998 Measuring the spin polarization of a metal with a superconducting point contact *Science* **282** 85–8
[22] Gambardella P, Rusponi S, Veronese M, Dhesi S S, Grazioli C, Dallmeyer A, Cabria I, Zeller R, Dederichs P H and Kern K 2003 Giant magnetic anisotropy of single cobalt atoms and nanoparticles *Science* **300** 1130–3
[23] Rusponi S, Cren T, Weiss N, Epple M, Buluschek P, Claude L and Brune H 2003 The remarkable difference between surface and step atoms in the magnetic anisotropy of two-dimensional nanostructures *Nat. Mater.* **2** 546–51